Improved Methods of Spillage Drag Prediction for Two-Dimensional Inlets

R. V. Osmon*
CETEC Corporation, Mountain View, Calif.

Semiempirical methods are presented which are directed toward more accurate prediction of spillage drag for two-dimensional inlets with swept side plates operating subcritically in the transonic flight regime. An empirically modified version of the linear bow-shock-position theory is compared with data and is shown to predict best the bow-shock position, with a similar improvement in the subcritical additive drag prediction. It is concluded that the error in predicting the subcritical additive drag of a supersonic inlet due to bow shock location by the linear theory can be significant at low supersonic Mach numbers. The cowl suction data of eight inlet cowls are correlated on a geometrical basis for freestream Mach numbers from 0.7 to 1.7. These correlations should be useful to the inlet designer by increasing the confidence level in making this estimation for two-dimensional inlets.

Nomenclature

A = area
A_c = inlet maximum capture area
A_{os} = stream-tube area bounded by inlet stagnation streamline surface and streamline passing through the bow-shock sonic points
A_{Rx} = projection of ramp area in the axial direction
A_s = sonic flow area between cowl and bow-shock sonic points
B = inlet width
C = $\beta\{\beta \tan\phi_s - (\beta^2 \tan^2\phi_s - 1)^{1/2}\}$
$C_{D_{add}}$ = additive drag coefficient, $D_{add}/q_\infty A_c$
c = chord
D_{add} = additive drag
D_{spill} = spillage drag
F_f = internal friction force
F_{int} = internal thrust
F_{net} = net thrust
F_{Rf} = external compression surface friction drag
G = empirical variable given in Fig. 6
i = MFR/MFR_{ref}
k = parameter defined by Eq. (18)
L = distance from inlet-plane to bow shock, see Fig. 2
M = Mach number
MFR = mass flow ratio, $(\rho A V)_i/\rho_\infty A_c V_\infty$
MFR_{ref} = reference or supercritical mass flow ratio
$\dot{m}$ = mass flow parameter, a function of Mach number
P = static pressure
P_T = total pressure
$P_{T_s}/P_{T_{os}}$ = average total pressure recovery through the hyperbolic portion of the bow shock between the stagnation streamline surface and the shock sonic point
S = bow-shock sonic point
SB = cowl sonic point
s_2 = distance stagnation streamline is above ramp surface for supersonic flow
t = thickness
V = velocity
$\dot{w}$ = flow rate, lb/sec
ww = inlet-plane height
z = general coordinate illustrated in Fig. 4
β = $(M^2 - 1)^{1/2}$
ΔC_{cc} = cowl suction coefficient = (maximum measured cowl drag − cowl drag)/$q_\infty A_c$
δ_s = local flow angle behind the bow-shock sonic point
H = angle sonic line makes with local vertical
η = parameter defined by Eq. (19)
θ_1 = first ramp angle
θ_2 = second ramp angle with respect to first
ρ = density
ϕ_s = shock angle for sonic downstream flow

Subscripts

e = effective
eq = equivalent
ex = exit
i = inlet-plane
R = ramp
t = throat
∞ = freestream

Superscript

$(\bar{\ })$ = average

Introduction

THE operation of a supersonic inlet at less than its maximum mass flow ratio is often required to permit the air induction system to supply the correct air flow to the engine. This may occur because of throttling back on the engines, or more likely because inlet design requirements conflict for takeoff, high subsonic cruise, and supersonic dash and therefore dictate a compromise in the inlet size. The amount of compromise depends entirely upon the particular aircraft, its missions, the engines, and the sophistication of the air induction system. Two important drag terms must be accounted for when estimating the performance of such a vehicle operating at less than its supercritical mass flow ratio. These are subcritical additive drag and the decrease in cowl drag commonly known as lip or cowl suction. The combination of the two is known as spillage drag.

Additive drag is not a drag in the ordinary sense. It is a simple but often misunderstood accounting method that corrects the net thrust as a function of engine operation and actual or presumed inlet flow conditions. The cowl suction is largely a function of cowl shape for a given mass flow ratio, and acts in the thrust direction to cancel some portion of the additive drag. It is analogous to the leading-edge suction of an airfoil.

Presented as Paper 67-449 at the AIAA 3rd Propulsion Joint Specialist Conference, Washington, D. C., July 17-21, 1967; submitted August 2, 1967, revision received January 16, 1968. The cooperation of NASA Ames in making the test data and shadowgraphs of Ref. 2 available is sincerely appreciated. In particular the author is grateful to W. E. Anderson of the Air Breathing Propulsion Branch for his helpful suggestions.

* Member of Senior Staff; original paper written while at Northrop Norair, Hawthorne, Calif. Member AIAA.

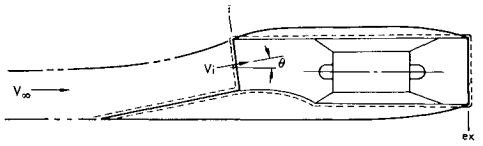

Fig. 1 Inlet-engine schematic.

In the preliminary stages of aircraft propulsion system design, many inlet configurations are likely to be considered for which an additive drag and cowl suction estimate must be made for each subcritical mass flow ratio in order to make a meaningful comparison of the performance of various design candidates. It is toward the more accurate prediction of these quantities that the following material is directed.

Definition of Spillage Drag

Spillage drag is defined here as additive drag minus cowl suction. It is a correction applied to net thrust to obtain the net propulsive thrust. Cowl suction is the decrease in cowl drag that occurs when an inlet operates at a mass flow lower than its reference value. As such, it is a function of inlet-engine operation for any given configuration and is logically included as a correction to the propulsion system thrust, not to the aircraft drag. Additive drag can be thought of as subtractive thrust since it must be subtracted from engine net thrust as described below.

An inlet-engine combination is represented schematically in Fig. 1. The thrust of the propulsion system is produced by the pressures acting on all the internal surfaces enclosed by the dashed lines in Fig. 1, i.e.,

$$\text{internal thrust, } F_{\text{int}} = \int_i^{\text{ex}} (P - P_\infty)dA_x - F_f \quad (1)$$

where A_x is the projected surface area and F_f is the internal friction force. An equivalent and more practical method of computing F_{int} is to write the momentum balance between inlet and exit; thus

$$F_{\text{int}} = [(P_{\text{ex}} - P_\infty)A_{\text{ex}} + (\dot{w}_{\text{ex}}/g)V_{\text{ex}}] - [(P_i - P_\infty)A_i \cos\theta + (\dot{w}_i/g)V_i \cos\theta + (\bar{P}_R - P_\infty)A_{Rx} + F_{Rf}] \quad (2)$$

(See Nomenclature for definition of terms.) Historically, engine manufacturers quote thrust values without specifying the detailed inlet geometry, and therefore the second bracketed term on the right of Eq. (2) is not known because V_i, A_i, $\bar{P}_R$, and A_{Rx} are functions of inlet geometry. To get around this problem, a "net" thrust has been defined,

$$F_{\text{net}} \equiv \int_\infty^{\text{ex}} (P - P_\infty)dA_x - F_f \quad (3)$$

The difference between Eqs. (1) and (3) is that the latter includes the pressure integral along the entering stagnation streamline. This may be rewritten using the momentum equation,

$$F_{\text{net}} = [(P_{\text{ex}} - P_\infty)A_{\text{ex}} + (\dot{w}_{\text{ex}}/g)V_{\text{ex}}] - [(\dot{w}_\infty/g)V_\infty] \quad (4)$$

where the first bracketed term is known as gross thrust and the second as ram drag. The net thrust as defined is a fictitious thrust since it ignores actual inlet flow conditions. Rewriting Eq. (3) and combining it with Eq. (1) yields

$$F_{\text{net}} = \int_\infty^i (P - P_\infty)dA_x + \int_i^{\text{ex}} (P - P_\infty)dA_x - F_f = \int_\infty^i (P - P_\infty)dA_x + F_{\text{int}} \quad (5a)$$

or

$$F_{\text{int}} = F_{\text{net}} - \int_\infty^i (P - P_\infty)dA_x \quad (5b)$$

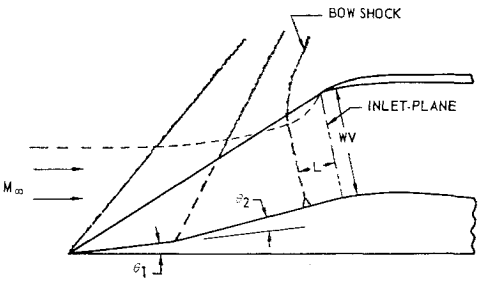

Fig. 2 Inlet geometry.

The second term on the right has been defined as the additive drag D_{add}. Utilizing the momentum equation again, D_{add} may be rewritten as

$$D_{\text{add}} = (P_i - P_\infty)A_i \cos\theta + (\bar{P}_R - P_\infty)A_{Rx} + (\dot{w}_i/g)(V_i \cos\theta - V_\infty) + F_{Rf} \quad (6)$$

The external compression surface friction drag F_{Rf} is usually relatively small and therefore is neglected. The spillage drag is

$$D_{\text{spill}} = D_{\text{add}} - \text{cowl suction} \quad (7)$$

and finally the net propulsive thrust may be defined as

$$F_{\text{net prop}} = F_{\text{net}} - D_{\text{spill}} \quad (8)$$

The ramp drag term $(\bar{P}_R - P_\infty)A_{Rx}$ of the additive drag in Eq. (6) requires an estimate for supersonic operation of the position of the subcritical bow shock in order to calculate the average ramp pressure $\bar{P}_R$. The bow-shock distance from the inlet-plane is denoted herein as L and is illustrated in Fig. 2. Methods available to determine the bow-shock position as a function of inlet mass flow ratio (MFR) and Mach number are covered in the following discussion.

Approximate Bow-Shock-Position Theories

The derivation of the continuity method of determining the expelled bow-shock location ahead of the inlet-plane is given by Moeckel.[1] The method has been referred to as the Moeckel theory and is derived for both plane and axially symmetric bodies. The theory for plane bodies is of concern here and is summarized below with modifications and definitions appropriate to inlets with external compression surfaces.

Figure 3 illustrates the inlet bow shock and basic nomenclature used in the Moeckel derivation. The Moeckel continuity method assumes the following. The supersonic flowfield and subsonic spillage behind the bow shock are one-di-

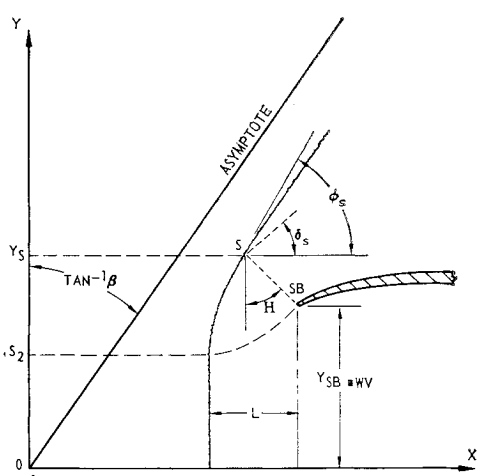

Fig. 3 Bow-shock-position notation.

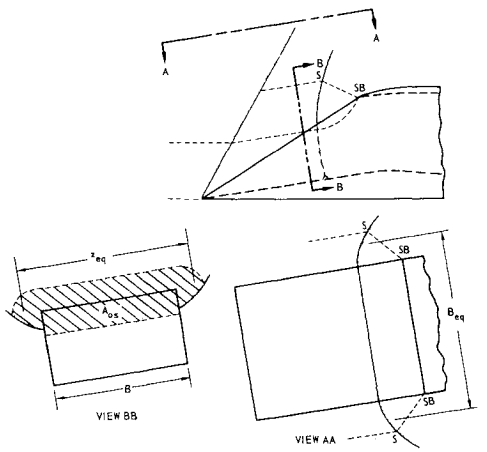

Fig. 4 Inlet flowfield.

mensional, and the bow-shock wave is hyperbolic in shape outboard of the stagnation streamline. The sonic line between the cowl and bow shock is linear and perpendicular to the deflected streamline at the shock sonic point. It is assumed here that the bow shock does not intersect an oblique shock in the mass flow range of interest, and that the shock is locally normal inboard of the stagnation streamline surface.

Two-dimensional inlets often have a three-dimensional flowfield externally, because the side plates must be of practical size or are nonexistent, depending on the inlet aspect ratio and inlet location. A common type of side plate configuration is the swept or triangular side plate shown in Fig. 4. It must be assumed, in this case, that some lateral spillage occurs, i.e., not all the spillage occurs over the cowl as in the idealized case of plane flow.

Equation (33) of Ref. 1 gives the nondimensionalized bow-shock position (BSP) as

$$(L/wv) = (y_s/wv)(C + \tan H) - C(s_2/wv) - \tan I \quad (9)$$

where C is a function of Mach number only. As shown in Fig. 3, s_2 locates the stagnation streamline surface and y_s locates the streamline that passes through the bow-shock sonic point. For plane flow, the angle that the sonic line makes with the local vertical H is assumed to equal the local flow deflection angle at the sonic point δ_s.

An expression for y_s/wv in terms of known parameters is sought. Looking at Figs. 3 and 4, the sonic flow area may be represented as

$$A_s = [(y_s - wv)/\cos\delta_s] \text{ (equivalent width, } B_{eq})$$

The stream-tube area of the mass flow entering the bow shock between the stagnation streamline surface and the streamline that intersects the bow-shock sonic point may be represented as

$$A_{os} = (y_s - s_2)(\text{equivalent lateral distance, } z_{eq})$$

and is shown as the shaded area in view BB of Fig. 4. The area ratio A_s/A_{os} then is

$$\frac{A_s}{A_{os}} = \frac{y_s - wv}{y_s - s_2} \cdot \frac{1}{(z/B)_{eq}} \cdot \frac{1}{\cos\delta_s} \quad (10)$$

where $(z/B)_{eq}$ is to be determined from experiment. Dividing through by wv and solving for y_s/wv

$$\frac{y_s}{wv} = \frac{1 - (z/B)_{eq}(s_2/wv)(A_s/A_{os})\cos\delta_s}{1 - (z/B)_{eq}(A_s/A_{os})\cos\delta_s} \quad (11)$$

from continuity, we have $\dot{w}_s = \dot{w}_{os}$, or

$$P_{Ts}A_s(P/P_T\mathring{m})_s = P_{Tos}A_{os}(P/P_T\mathring{m})_{os}$$

and therefore

$$\frac{A_s}{A_{os}} = \frac{1/[P_{Ts}/P_{Tos}]}{(A/A^*)_{os}} \quad (12)$$

where P_{Ts} is the average total pressure of the sonic flow.[1] Substituting Eqs. (12) and (11) into (9) and rearranging, the nondimensionalized bow-shock-position equation is obtained,

$$\frac{L}{wv} = \left[1 - \frac{s_2}{wv}\right] \frac{C + [z/B]_{eq}(A_s/A_{os})\sin\delta_s}{1 - [z/B]_{eq}(A_s/A_{os})\cos\delta_s} \quad (13)$$

For inlets with infinitely large side plates $(z/B)_{eq} = 1$ and s_2/wv becomes the ratio of mass flow to the supercritical value, yielding

$$\frac{L}{wv} = \left[1 - \frac{MFR}{MFR_{rcf}}\right] \frac{C + (A_s/A_{os})\sin\delta_s}{1 - (A_s/A_{os})\cos\delta_s} \quad (14)$$

All terms on the right side of Eq. (14) are functions of the plane supersonic flowfield Mach number except for MFR, which is the independent variable. Therefore, once Mach number is established, the predicted bow-shock position is a linear function of MFR. Equation (14) corresponds to Eq. (36) of Ref. 1 and predicts the bow-shock position for two-dimensional inlets having a plane supersonic flowfield.

Access to shadowgraph data generated in the test of Ref. 2 permitted an empirical approach to be taken with regard to $(z/B)_{eq}$ for a two-dimensional inlet with swept side plates. It was noted in analyzing bow-shock-position data that the negative slope of the L/wv data generally decreased with MFR. Extrapolation of the data to the fictitious condition of zero mass flow indicated the slope could be quite small. Since the slope cannot become positive, zero slope at zero mass flow ratio is a definite possibility. The approach taken to find an empirical equation that would allow prediction of BSP for this type of inlet was as follows: 1) Let $s_2/wv = MFR/MFR_{ref} = i$ in Eq. (13), and let $(z/B)_{eq}$ be replaced by an effective value $(z/B)_e$. 2) Assume the slope of the curve defined by L/wv vs i is zero at $MFR = 0$. 3) Find an expression for $(z/B)_e$ that satisfies the boundary conditions $d(L/wv)/di = 0$ at $i = 0$ and $(z/B)_e = 1$ at $i = 1$.

The simplest form of $(z/B)_e$ that satisfies the two boundary conditions is

$$(z/B)_e = k - (1 - i)/\eta \quad (15)$$

where $k = 1$, and η is a number to be determined from the boundary conditions and the supersonic flowfield Mach number. The bow-shock-position equation then becomes

$$\frac{L}{wv} = (1 - i)\frac{C + \{k - (1 - i)/\eta\}\, A_s/A_{os}\sin\delta_s}{1 - \{k - (1 - i)/\eta\}\, A_s/A_{os}\cos\delta_s} \quad (16)$$

Once the relevant supersonic flowfield Mach number is established, η can be solved for by setting

$$[d(L/wv)]/di = 0 \qquad \text{and letting} \qquad i \to 0$$

which yields

$$\eta = \frac{E \pm [E(E + CF)/(1 - kF)]^{1/2}}{kE + C} \quad (17)$$

where

$$E = (A_s/A_{os})\sin\delta_s \qquad \text{and} \qquad F = (A_s/A_{os})\cos\delta_s$$

Take the positive root since the negative root gives negative (L/wv) values which have no physical significance.

Knowledge of the amount of mass flow loss (relative to plane supersonic flow) through supersonic spillage is not necessary when using Eq. (16) since i is the ratio of mass flow to the supercritical value. However, the three-dimensional-

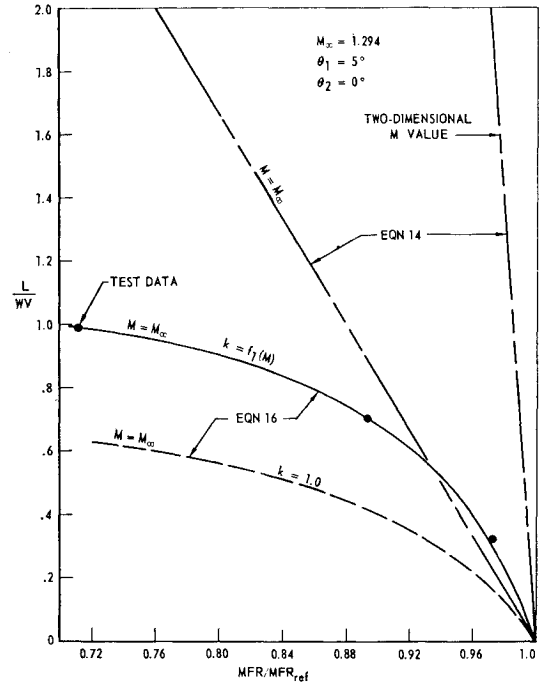

a)

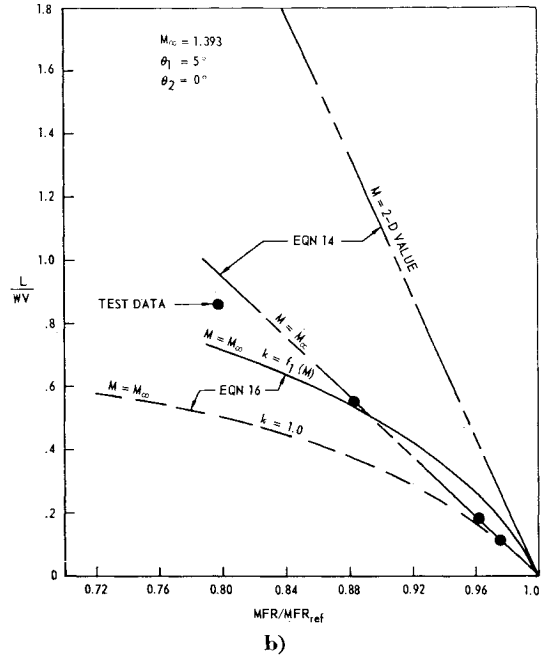

b)

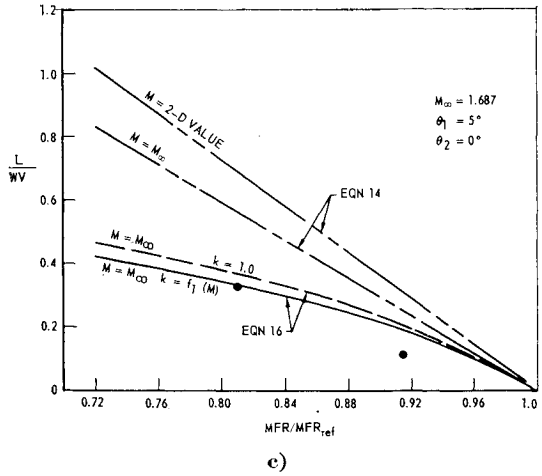

c)

Fig. 5 Bow-shock position.

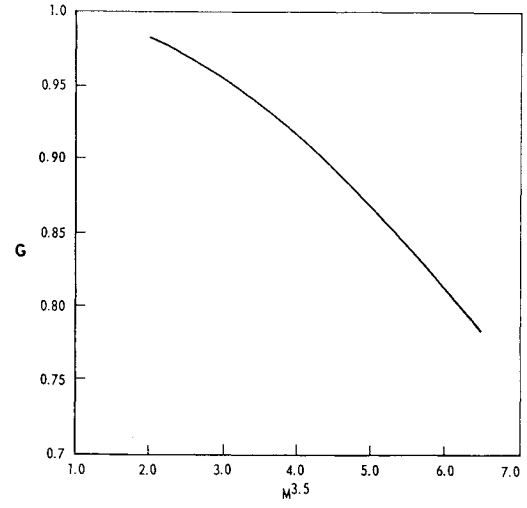

Fig. 6 Empirical variable G [for use in Eqs. (18) and (19)].

ity of the local supersonic flowfield just ahead of the hyperbolic portion of the bow shock should be considered in establishing the relevant Mach number for the BSP calculation. Three-dimensional effects are highly dependent upon configuration and freestream Mach number and must be estimated individually.

Comparison of Bow-Shock-Position Data with Prediction Methods

Equation (16) is plotted as the dashed line in Figs. 5a–5c for $k = 1$ and is compared with shadowgraph data from the test of Ref. 2. The rectangular inlet model has double-wedge external compression surfaces with swept side plates and a constant area section aft of the inlet-plane. The first ramp angle is 5° and the second (variable) ramp is set at 0° relative to the first, yielding an effective single 5° wedge. From Mach cone considerations, the relevant Mach number used to determine C, δ_s, and A_s/A_{os} in Eq. (16) was approximated to be the freestream value for these cases. In other words, because of the geometry of the inlet, the compressed flow behind the oblique shock wave expanded back to the freestream Mach number in the area of the hyperbolic portion of the bow shock.

The characteristic trend of the data is predicted reasonably well for $k = 1$, but the absolute level generally is not. Equation (14) (linear theory) is also compared with the data for the cases of the relevant Mach number being the two-dimensional and the freestream values. The data of Fig. 5b are predicted quite well by Eq. (14) with $M = M_\infty$; however, the data of Figs. 5a and 5c are not. The problem of predicting the absolute level of the data with Eq. (16) was solved by allowing k to vary as an empirical function of the relevant Mach number. Values of k that would best satisfy all three sets of data ranged from 0.978 to 1.04, and can be obtained from the empirical equation

$$k = G/F = f_1(M) \tag{18}$$

where $G = f_2(M^{3.5})$ as shown in Fig. 6. The solid line in Figs. 5a–5c is obtained by letting $k = f_1(M)$. It fits the data quite satisfactorily in Figs. 5a and 5c and less so in Fig. 5b, although the absolute level is reasonable now. Equation (17) may be revised to

$$\eta = \frac{E + [E(E + CF)/(1 - G)]^{1/2}}{G(E/F) + C} \tag{19}$$

The use of Fig. 6 and Eqs. (16, 18, and 19), together with a judgment of the relevant inlet flowfield Mach number, should give increased confidence to the prediction of bow-shock position for this type of inlet. Since the correlation is based on

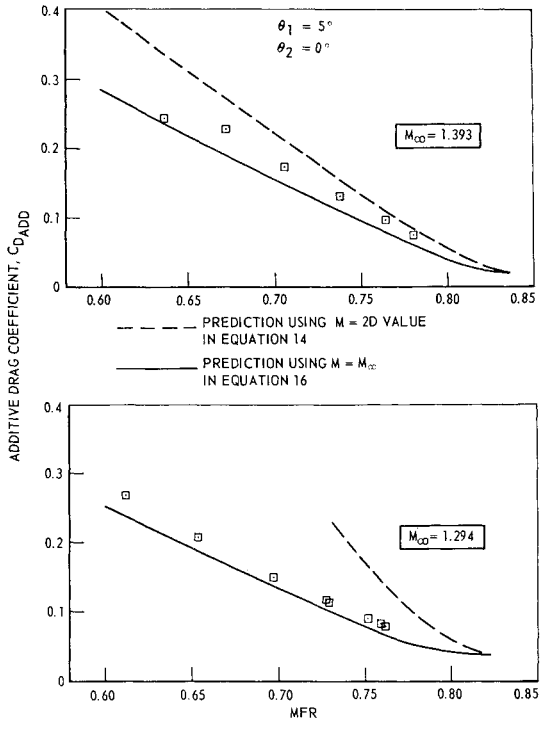

a)

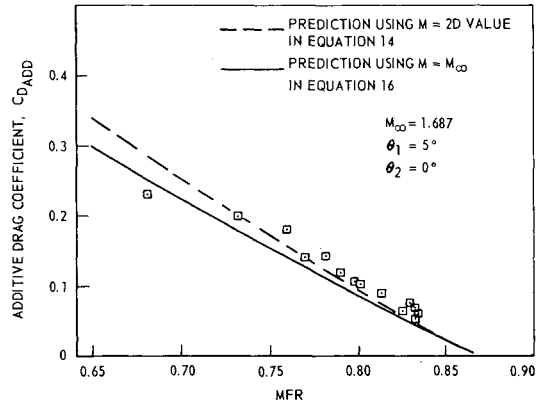

b)

Fig. 7 Additive drag coefficient.

limited (but hitherto unavailable) data, it should be checked against future data or data unknown to this writer. The effect of bow-shock position on the prediction of additive drag is discussed in the following section.

Effect of Bow-Shock Position on Predicted Additive Drag

The additive drag coefficient data corresponding to the bow-shock data of Figs. 5a–5c are presented in Figs. 7a and 7b. The solid line is the additive drag predicted by locating the bow shock according to the method previously described; the dashed line is the predicted additive drag using Eq. (14). Both curves use one-dimensional theory to predict the additive drag coefficient independent of the method of locating the bow shock. The average ramp pressure behind the bow shock is taken as one-half the sum of the inlet-plane static pressure plus the static pressure behind a normal shock. It is clear that the predicted additive drag can be significantly in error if the linear bow-shock equation is used, especially at the lower freestream Mach numbers. Note that the error at Mach 1.29 in Fig. 7a would result in a (fictitious) penalty being given to the propulsion system. The difference between the solid line and the data reflects shortcomings in other parts of the additive drag theoretical model. For instance, the theory used here assumes the bow shock is locally normal, whereas in fact it is observed to be a strong oblique shock with a lambda foot—the result of viscous interaction effects. Improvements in the theory in this regard would move the predicted (solid line) curves toward the data.

Figure 7b indicates the sensitivity of the additive drag prediction to bow-shock position decreases as the Mach number increases. Although the bow shock is overpredicted at Mach 1.69 by 100 to 150% using the two-dimensional Mach number in Eq. (14), the additive drag is generally well predicted. Definite improvements in the additive drag prediction at the lowest of the three freestream Mach numbers are obtained by using either the semiempirical or linear bow-shock methods when consideration is given to the relevant Mach number.

Cowl Suction

The decrease in cowl drag due to inlet operation below its reference mass flow is known as cowl or lip suction. It acts in the thrust direction, and, as shown previously, an estimate of cowl suction is necessary for the prediction of spillage drag. The size of the suction coefficient is generally small relative to the additive drag coefficient for inlets designed for both supersonic and subsonic operation. Nevertheless, its exact size is difficult to predict from theory with much confidence.

Cowl suction coefficient data were obtained from pressure measurements by Petersen and Tamplin[2] for ten cowl geometries, several ramp angle combinations, and three side plate geometries at Mach 0.69, 0.85, 1.09, 1.29, 1.39, and 1.69. A semiempirical approach was taken herein in an effort to correlate the suction data based on known geometrical and inlet flow parameters. The geometries studied are summarized in Fig. 8. The resultant cowl suction coefficient ΔC_{c_c} correlations for each nominal test Mach number are presented in Fig. 9.

The cowl drag increment parameter combines effective thickness-to-chord ratios t/c for both the cowl and the ramp, projected capture area A_c, maximum projected inlet area A_{max}, and the incremental cowl drag coefficient (or suction coefficient) based on capture area. Effective cowl thickness

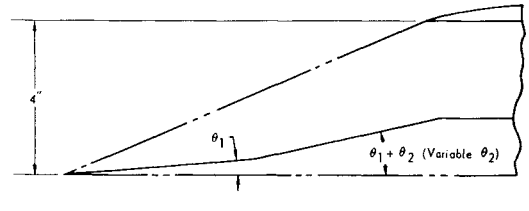

RAMP	θ_1	DESIGN M_∞
R1	5°	3.0
R2	7°	3.0
R3	12°	3.0
R4	5°	2.2

NOTE: INLET WIDTH IS 4"

COWL	TYPE	INITIAL ANGLE, ϕ ~DEG	LIP RADIUS ~INCHES	CHORD, c ~INCHES	THICKNESS, t ~INCHES
C1	CIRCULAR	10	0	5.71	0.5
C5	ARC	15	0	3.79	0.5
C6	↓	15	0	7.59	1.0
C7		10	0.04	5.71	0.5
C8		10	0.10	5.71	0.5
C2	WEDGE	6	0	4.76	0.5
C3	↓	10	0	2.84	0.5
C4		15	0	1.87	0.5

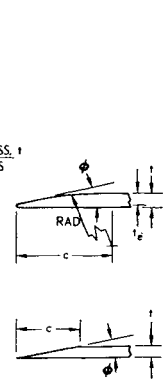

Fig. 8 Summary of test model hardware.

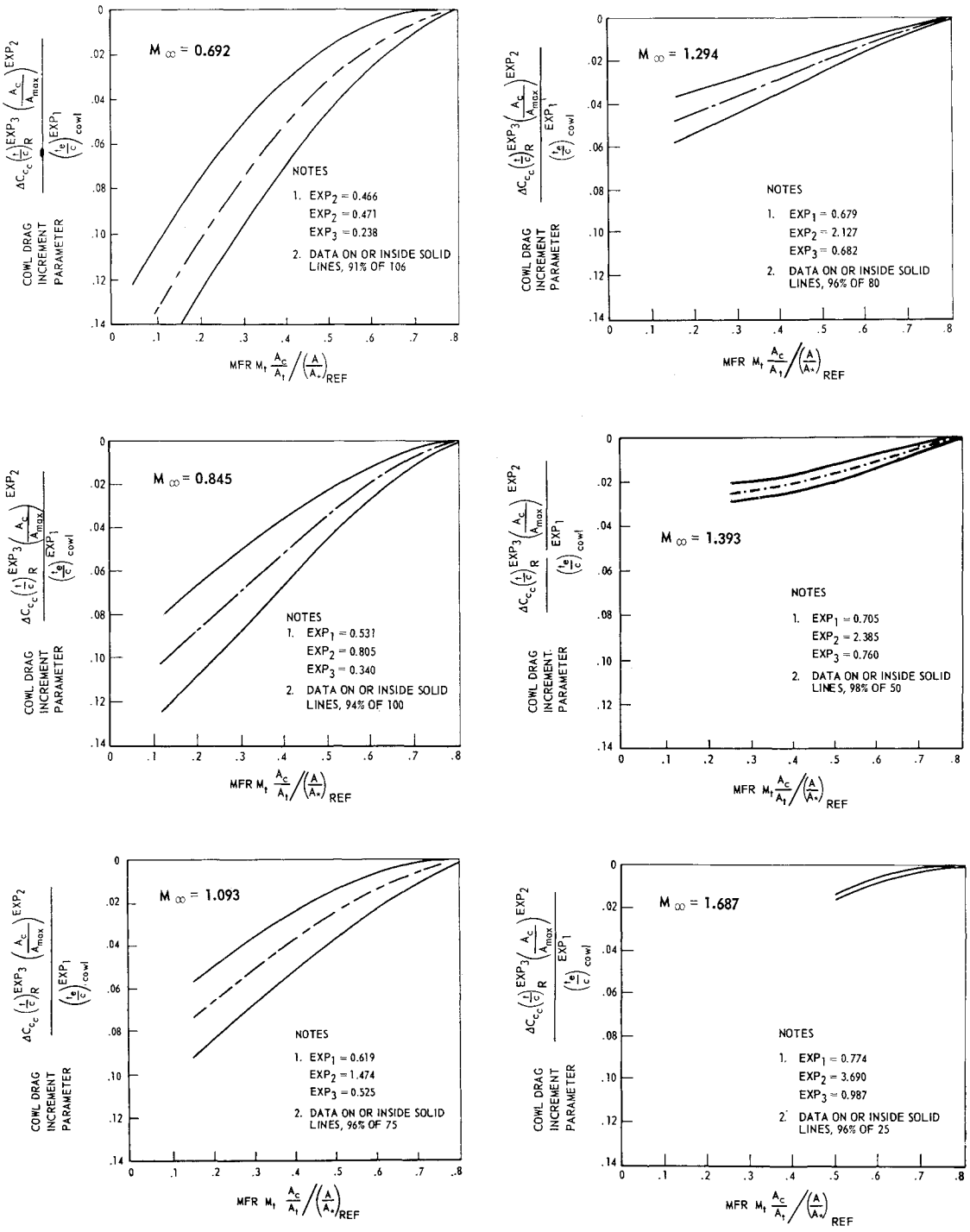

Fig. 9 Cowl suction correlation.

is illustrated in Fig. 8; it is defined as the physical thickness minus the lip radius. The ramp effective thickness-to-chord ratio is the tangent of the average ramp angle weighted on a length basis. The exponents (1, 2, and 3) are empirical functions of freestream Mach number only and are listed on each correlation.

The abscissa is a parameter proportional to the inlet momentum (mV) and includes mass flow ratio (MFR), throat Mach number, capture-to-throat area ratio, and the contraction ratio required to decelerate a reference flow to sonic velocity isentropically, A/A^* (see Ref. 3). Subsonically, A/A^* corresponds to freestream Mach number. Supersonically A/A^* corresponds to the external Mach number to which the flow is assumed to expand at the end of the cowl area change. The flow at this point is assumed to have freestream static pressure and stagnation pressure that corresponds to the recovery through the inlet oblique shock waves plus a normal shock.

The slope of the cowl suction correlations is high at the low test Mach numbers and decreases as Mach number increases. Also, the ability to collapse the data onto a narrow band is seen to increase with Mach number. The correlations allow cowl suction coefficient values to be computed for the geometries of the test model, and it seems reasonable to expect the correlations to be valid for other two-dimensional inlets. The values obtained can be combined with additive drag to predict the spillage drag of an inlet having a specific cowl shape. The geometrical limits of the correlations are not known at this time; however, a prediction outside the geometric variables of the test model certainly could be made

without undue concern as long as the excursion is reasonable. Other existing data should be compared with the correlations to help determine the extent of applicability. If mixed compression is involved, the throat Mach number and area should be replaced by appropriate inlet-plane values. In any case, the correlations should permit an increased level of confidence in predicting cowl suction for this and other two-dimensional inlets designed for both supersonic and subsonic operation.

Conclusions

1) The linear bow-shock-position theory in conjunction with the plane supersonic inlet-flowfield Mach number has been shown to overpredict the bow-shock position of a two-dimensional inlet with swept side plates. 2) An empirical modification of the linear theory has been made that predicts the bow-shock position of the test model with reasonable consistency. 3) Possible three-dimensional flow effects in the external supersonic flowfield of a two-dimensional inlet must be considered when selecting a reference Mach number for computing bow-shock position. 4) The error in predicting the additive drag of a supersonic inlet due to inaccurate bow-shock location at low supersonic Mach numbers can be significant. 5) Cowl suction correlations not previously available have been produced from experimental data that should be useful to the inlet designer and should increase the confidence level in making this estimate for two-dimensional inlets.

References

[1] Moeckel, W. E., "Approximate Method for Predicting Form and Location of Detached Shock Waves Ahead of Plane or Axially Symmetric Bodies," TN 1921, July 1949, NACA.

[2] Petersen, M. W. and Tamplin, G. C., "Experimental Review of Transonic Spillage Drag of Rectangular Inlets," Rept. NA-66-10, North American Aviation Inc.; U.S. Air Force Rept APL-TR-66-30, May 1966.

[3] Ames Research Staff, "Equations, Tables, and Charts for Compressible Flow," Rept. 1135, 1953, NACA.

MAY-JUNE 1968 J. AIRCRAFT VOL. 5, NO. 3

Structure of Trailing Vortices

BARNES W. MCCORMICK*
The Pennsylvania State University, University Park, Pa.

JAMES L. TANGLER†
U.S. Army, San Francisco, Calif.

AND

HAROLD E. SHERRIEB‡
LTV Aerospace Corporation, Dallas, Texas

A study of aircraft trailing vortex systems, involving actual flight testing as well as model testing and analytical considerations, has resulted in a method for predicting the vortex geometry and velocity field downstream of an aircraft. It is found that the vortex decay can be described by geometric similarity considerations and not by any modification of the Navier-Stokes equations. This conclusion is based on detailed velocity measurements made through the vortex immediately behind a test aircraft up to distances of approximately 1000 chord lengths downstream of the aircraft. This report includes a presentation of the data on which the conclusions are based, as well as a description of test equipment and procedures.

Nomenclature

a = core radius [radius where $v(r)$ is a maximum]
a_0 = initial value of the core radius immediately behind the wing
b = wing span
c_0 = midspan chord
$\bar{c}$ = mean chord = S/b
E = kinetic energy of vortex system/unit length
n = exponent in vorticity distribution, Eq. (23)
r = radial distance from center of vortex; also coordinate coincident with vortex radius but arbitrary origin (Fig. 9)
r_∞ = pseudo-radius where $\Gamma(r) = \Gamma_\infty$
S = wing planform area
t = time
t' = dimensionless time, Eq. (8)
$v(r)$ = tangential velocity at radius r
v = maximum value of $v(r) = v(a)$
v_0 = value of v immediately behind the wing
V = aircraft velocity
w = half-radius = r at which $\zeta = \zeta_0/2$
w_0 = value of w for $t = 0$
Y = distance along line through vortex center
Z = distance downstream of wing trailing edge
$\gamma(2/n)$ = gamma function with argument $(2/n)$
Γ = circulation at any radius
Γ_∞ = total circulation (as $r \to \infty$)
ν = kinematic viscosity
ν_e = effective kinematic viscosity
ω = angular velocity of fluid
ω_v = angular velocity of vanes
ζ = vorticity at any radius
ζ_0 = center value of $\zeta(r = 0)$
ζ_{0I} = value of ζ_0 immediately behind wing

Received October 19, 1967; revision received January 31, 1968. This project was supported by the U.S. Army Research Office (Durham) under Contract DA-31-124-ARO (D)-149. Our appreciation is extended to D. M. May, A. H. Logan, T. L. Grow, and H. Smith for their contributions.

* Professor of Aerospace Engineering. Associate Fellow AIAA.
† Captain.
‡ Aerodynamics Design Engineer. Associate Member AIAA.